A mathematical model for the dynamic angle of repose of a granular material in the rotating drum

Pourandi, Sahar; van der Sande, P. Christian; Weinhart, Thomas; Ostanin, Igor

DOI
10.1016/j.powtec.2024.120176

Publication date
2024

Document Version
Final published version

Published in
Powder Technology

Powder Technology 446 (2024) 120176

Contents lists available at ScienceDirect

Powder Technology

journal homepage: www.journals.elsevier.com/powder-technology

A mathematical model for the dynamic angle of repose of a granular material in the rotating drum

Sahar Pourandi [a,*], P. Christian van der Sande [b], Thomas Weinhart [a], Igor Ostanin [a]

[a] University of Twente, Drienerlolaan 5, Enschede, The Netherlands
[b] Delft University of Technology, Van der Maasweg 9, Delft, The Netherlands

HIGHLIGHTS

- We offered an analytical model for the dynamic angle of repose in a rotating drum.
- We calibrated our model using discrete element simulations.
- The model was validated using the lab-scale experiment.

GRAPHICAL ABSTRACT

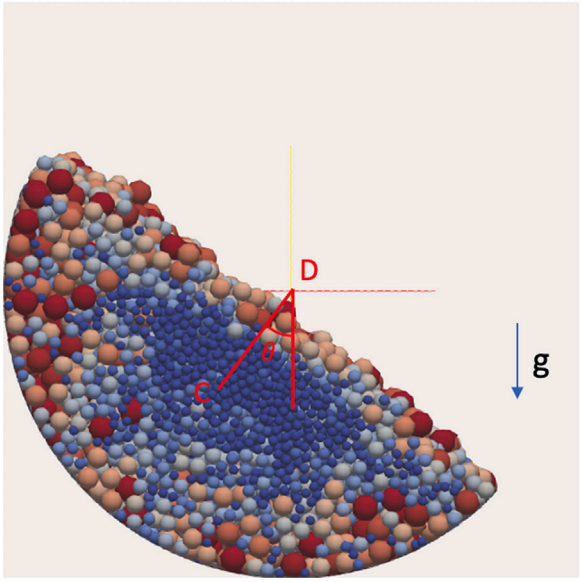

ARTICLE INFO

Keywords:
Granular flow
Dynamic angle of repose
Discrete element method

ABSTRACT

This study introduces a mathematical model to predict the dynamic angle of repose exhibited by granular materials in a rotating drum. The model accounts for the effect of particle properties, particularly sliding and rolling friction, as well as process conditions, i.e., the Froude number. We show that the effects of particle properties can be modeled independently of the process conditions, resulting in a multiplicative model. The model is validated using experimental data taken at different Froude numbers, yielding favorable agreement between the predicted dynamic angle of repose and the experimental observations. The findings of this study hold significant implications for engineering disciplines, as they provide crucial insights for optimizing processes involving granular materials in various engineering applications.

* Corresponding author.
E-mail addresses: s.pourandi@utwente.nl (S. Pourandi), p.c.vandersande@tudelft.nl (P.C. van der Sande), t.weinhart@utwente.nl (T. Weinhart), i.ostanin@utwente.nl (I. Ostanin).

https://doi.org/10.1016/j.powtec.2024.120176
Received 11 March 2024; Received in revised form 30 July 2024; Accepted 11 August 2024
Available online 12 August 2024

1. Introduction

Granular materials, such as sand, powders, and grains, exhibit distinctive characteristics due to their discrete nature and interparticle interactions. Understanding the dynamics and flow behavior of granular materials is crucial in various research fields, including engineering and materials science. The static and dynamic angles of repose (AoRs) are common measures to characterize a granular material. The static AoR represents the maximum stable angle at which a pile of granular material can maintain its shape without collapsing or flowing. This is typically measured in the heap test [1] , [2], see Fig. 1 (left). On the other hand, the dynamic AoR is defined as the angle at which the material flows. Typically, dynamic AoRs are determined by allowing granular material to flow down a sloping surface at a controlled speed or observing it during dynamic processes such as rotating or conveying. The dynamic AoR is typically measured in the rotating drum [2], see Fig. 1 (right).

The dynamic AoR shows the material's flow behavior in the presence of external forces, whereas the static AoR displays the material's inherent stability. While the static AoR has been extensively studied, the dynamic AoR remains a challenging yet essential area of investigation.

Early research on granular materials was primarily focused on the static AoR, which determines the stability of granular piles without external forces. Miura et al. [1] studied the static AoR of sands. They found that increasing the amount of material or the size of the conical heap decreases the AoR. Furthermore, they observed that decreasing the pouring rate of granular material increases the static AoR. Elekes et al. [3] proposed a theoretical expression for the static angle of repose as a function of particle size and gravity. Their particle-based numerical models considered sliding and rolling resistance and van der Waals forces. Moreover, they discovered that heaps undergo a shift from conical to irregular shapes when the ratio of cohesive to gravitational force exceeds a critical value. This finding provided a surrogate for particle-scale interactions derived from heap morphology.

In recent years, increasing interest has been in understanding granular material dynamics. Several studies have explored the effects of external forces on the AoR. The study by the French research group Groupement de Recherche Milieux Divisés (GDR MiDi) [4] explored the influence of continuous shear deformation on the dense granular flow. This work identified relevant timescales, length scales, and transitions between flow regimes using data from experiments and simulations across various geometries. In addition, it highlighted the importance of considering non-local rheology in granular material dynamics. Linz and Hanggi [5] studied the influence of vibration on the dynamic AoR in granular systems. In this work, the avalanche dynamics on quasi-two-dimensional granular surfaces in response to vertical vibration was investigated, and the relation between vibration characteristics and the minimum AoR was suggested. Kleinhans et al. [6] investigated the effect of gravity on both the dynamic and static angles of repose using rotating drums. According to their experiments, the static angle of repose of granular material increases under low gravity while the dynamic angle of repose decreases, leading to larger-volume avalanches. These results contradict earlier findings and the commonly held belief that these angles do not depend on gravity. It should be noted that Kleinhans et al.'s conclusions apply to particles between the dimensions of 0.2 and 2.4 mm, with smooth spherical particles as well as angular particles and air and water as interstitial fluids.

Sliding and rolling friction play an important role in granular material dynamics. According to Zhou et al. [7], for coarse sphere glass beads, static AoR increases with the increase of both the sliding and rolling friction coefficients. Using discrete element method (DEM) simulations, Santos et al. [8] examined the effect of sliding friction on the dynamic AoR in a rotating drum. It was confirmed that the dynamic AoR increases with the sliding friction coefficient. Briend et al. [9] showed that the AoR of the soil increases with the rolling friction coefficient; similar findings have been reported in [10,11]. Markauskas and Kačianauskas [12] used a DEM simulation that included rolling friction to represent the flow of ellipsoidal rice grains. It was demonstrated that the presence of rolling friction is crucial for the correct prediction of the dynamic AoRs. In summary, it is reliably established by many authors that the dynamic AoR increases with the increase of sliding and rolling friction coefficients.

Considering the drum feature of rotation speed, both Liu et al. [13] and Yang et al. [14] studied the effect of drum rotation on the AoR. Liu et al. [13] conducted experiments to measure the upper and lower angles of glass beads in a rotating drum. They examined the effect of rotation speed, fill level, and drum diameter on the lower and upper angles. They observed that rotation speed and the fill level have negligible effects on these two angles. Moreover, Yang et al. [14] found that the dynamic AoR increases linearly with the rotation speed.

Our work aims to establish a mathematical model that predicts the dynamic AoR by considering particle properties, such as sliding and rolling friction, and the process property of drum rotation speed. Such a model would be able to analyze and predict the behavior of granular materials under dynamic settings and can offer interesting insights valuable for process optimization. The model relies on the data obtained in the numerical simulations of rolling and cascading of polydisperse spherical particle assemblies in the rotating drum. The model of particle interaction assumes elastic frictional contacts and zero adhesion between the particles. The DEM model utilizes spherical particles; the effects of increased particle resistance to rolling due to aspherical particle shapes are represented effectively with the rolling friction included in the contact model. The particle size distribution and bulk density used in the DEM model were extracted from the characterization experiment carried out with the industrial-grade polypropylene powder.

The paper is structured as follows. Section 2 describes the methodologies used, including the characterization of the polypropylene powder, DEM model, simulation and experiment setup, and the method to measure the dynamic AoR in both simulation and experiment. Afterward, Section 3 presents the obtained results and the developed mathematical model. Finally, Section 4, summarizes the main points of this work.

2. Methods

2.1. Particle characterization

An industrial-grade polypropylene reactor powder was chosen as the model granular material for this study. This particulate was used in the experiment; the corresponding properties were assigned to the particles in the simulation. The volume-based particle size distribution of the polypropylene powder was acquired by laser diffraction with the Coulter LS230 particle size analyzer. The particle size distribution is presented graphically in Fig. 2 and in tabulated form in Table 1. The aerated (loose) bulk density was experimentally measured following Carr's study [15]: The material was screened through a funnel into a 100 mL glass cylinder till overflowing. The overflow was leveled off, and the weight of the container was measured. After subtraction of the weight of the empty cylinder, the aerated bulk density of the material was calculated, shown in Table 2. The elastic and shear modulus values for polypropylene were obtained from the material database provided by DesignerData.nl [16], and the coefficient of restitution was a typical value, shown in Table 2.

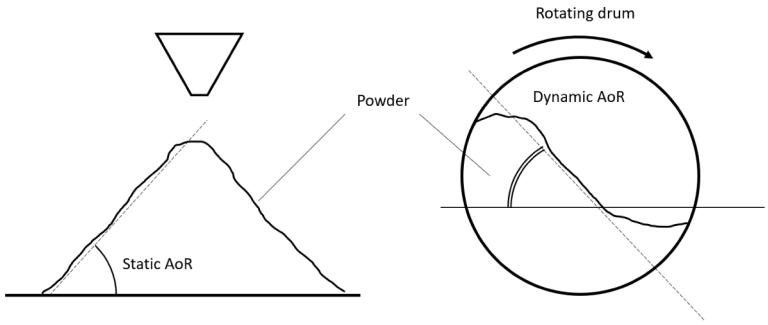

Fig. 1. Methods of measurement of static (left) and dynamic (right) AoR (after [2]).

Table 1
Particle size distribution.

Particle diameter (μm)	Cumulative volume (%)
506.0	10
712.7	25
904.6	50
1123	75
1345	90

Table 2
Material properties of the polypropylene particles.

Parameter	Value
Elastic modulus E	1.325×10^9 Pa
Shear modulus ν	4×10^8 Pa
Coefficient of restitution e	0.5
Aerated (loose) bulk density ρ	368 kg/m^3

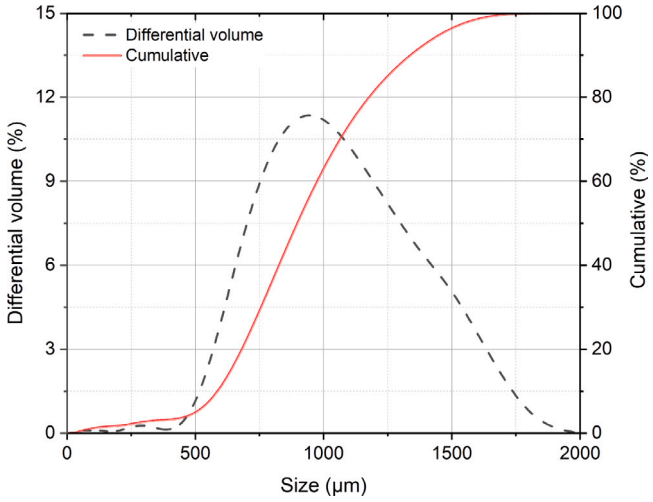

Fig. 2. Particle size distribution of the industrial-grade polypropylene material measured with the Coulter LS230 particle size analyzer.

2.2. Validating experiment

The dynamic AoR was measured using an in-house rotating drum setup. The setup consists of a rotating drum, an optical camera connected to a computer, and an LED panel. The drum has a length of 18 cm and a diameter of 14 cm. The drum is comprised of stainless steel with transparent polycarbonate windows on both sides. The drum was placed on two wheels that were rotated at the desired rotating speeds using a 60 W VEVOR motor. In this study, the drum was operated at 5, 10, 20, and 30 rpm rotation speeds. An LED panel was used to illuminate the front of the flowing material in order to induce contrast during the image acquisition. For each experiment, 426.9 g of polypropylene material was loaded in the drum, yielding a fill grade of 40%. Then, the drum was rotated at the desired rotation speed. After 30 s, the material flowing layer was conditioned at the desired rotation speed, and images of the flowing layer were acquired using a BASLER optical camera equipped with a 25 mm lens for a duration of 5 s with an image acquisition frame rate of 100 Hz.

Measurement of the dynamic AoR. We collected experimental data by recording videos of rotating drums and used image processing techniques to extract the required measurements. We determined the AoR by measuring the angle between the line connecting the drum's center and the powder's center and a vertical line, see Fig. 3.

2.3. Simulation

Our mathematical model relies on a large array of numerical simulations. To simulate the rotating drum, we used the discrete element method (DEM) [17]. With DEM, one can represent individual particles as discrete entities and accurately capture their interactions and motions within the drum. The simulations were performed using the software package MercuryDPM [18]. A contact model combining the Hertz–Mindlin [19] and the rolling friction contact models [20] was chosen to conduct the DEM simulations of the rotating drum. The rolling model is a linear model that considers dissipation in addition to elasticity. In the rolling friction model, the rolling stiffness is set equal to the stiffness used in the Mindlin model, so the rolling stiffness and tangential stiffness have the same units.

Simulation procedure. In DEM simulation, it is assumed that the AoR is influenced primarily by the contact parameters sliding coefficient of friction μ_s and rolling coefficient of friction μ_r. Since, for simplicity, we chose spherical particles to simulate non-spherical real particles in the DEM, the coefficient of rolling friction must consider the shape of the real particles [21], [22]. Therefore, in the DEM, rolling friction coefficients are considerably greater than for perfectly spherical particles [21].

Simulations for sliding and rolling coefficient of friction values ranging from 0.05 to 1, with 0.05 increments between particles, were performed. On the other hand, we considered the value of infinity[1] for sliding and rolling friction coefficients between the particles and the rotating wall while considering the value of zero for sliding and rolling friction coefficients between particles and the front and back walls.

The simulations were repeated at various rotation speeds to evaluate the influence of the flow regime, which is usually characterized by the dimensionless Froude number [24,25]. It is given by

$$Fr = \sqrt{\frac{\omega^2 D}{2g}} \tag{1}$$

[1] By infinity, we mean here a "machine" infinity and the corresponding numerical constant defined in C++ 11 standard [23].

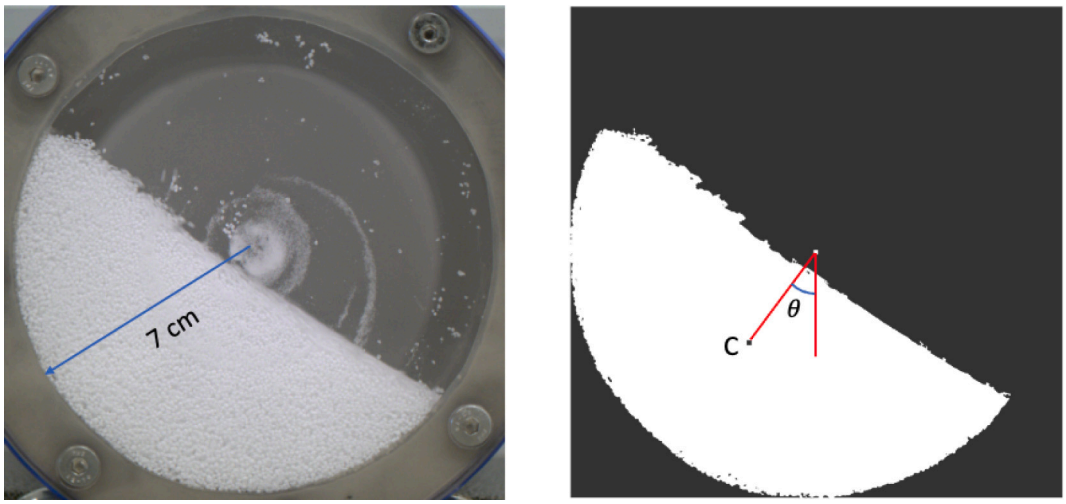

Fig. 3. Measurement of AoR of powder in the experimental rotating drum using image processing.

Table 3
Drum rotation speeds and their corresponding Froude numbers.

Rotation speed (rpm)	Froude number
5	0.0442
10	0.0885
20	0.1769
30	0.2654

Here, ω is the rotation speed of the drum, D is its diameter, and g is the gravitational acceleration. In our simulations, we studied the rolling and cascading regimes within a Froude number range of 0.04 to 0.3. Table 3 shows the rotation speeds used in our simulations and their corresponding Froude numbers.

In total, 1600 ($4 \times 20 \times 20$) simulations were performed for varying drum rotation speed, and coefficients of sliding and rolling friction. This broad parameter study allowed us to draw conclusions about the effect of friction on the dynamic AoR.

In all DEM simulations, we filled 40% of the rotating drum volume, which was 18 cm in length and 14 cm in diameter, with the particles corresponding to particles of an industrial polypropylene powder. We set the density such that we got the same bulk density in the experimental procedure. We increased the size of all particles by a factor of 5. This change enabled us to achieve shorter simulation times while correctly reflecting the system's fundamental dynamics and behavior; the drum size was about 30 times larger than the median particle diameter [26].

For every simulation parameter set, we performed a full-depth drum simulation; drum slicing or transverse periodic boundary conditions were not used to avoid the computationally expensive parametric studies necessary to establish the representative thickness of the slice in every flow regime.

The appropriate choice of the simulation time step Δt can speed up a simulation. Following [27], we used the simulation time step of 20% of $\Delta t_{\text{Rayleigh}}$ in our simulations to ensure numerical stability. $\Delta t_{\text{Rayleigh}}$ indicates the time scale corresponding to the propagation of elastic waves through the particles [28]. It is given by

$$\Delta t_{\text{Rayleigh}} = \frac{\pi R \sqrt{\frac{\rho}{G}}}{0.1631\nu + 0.8766} \tag{2}$$

Here, R, G, ν, and ρ are the smallest particle's radius, shear modulus, Poisson's ratio, and density, respectively. Moreover, the simulation time step can be increased significantly with no effect on stability, particle flow, and AoR by decreasing the stiffness of particles [29,30]. Following the guidelines in [29,30], we reduced the shear modulus of the particles in our DEM model by a factor of 10^3, leading to $10^{3/2}$ faster simulations.

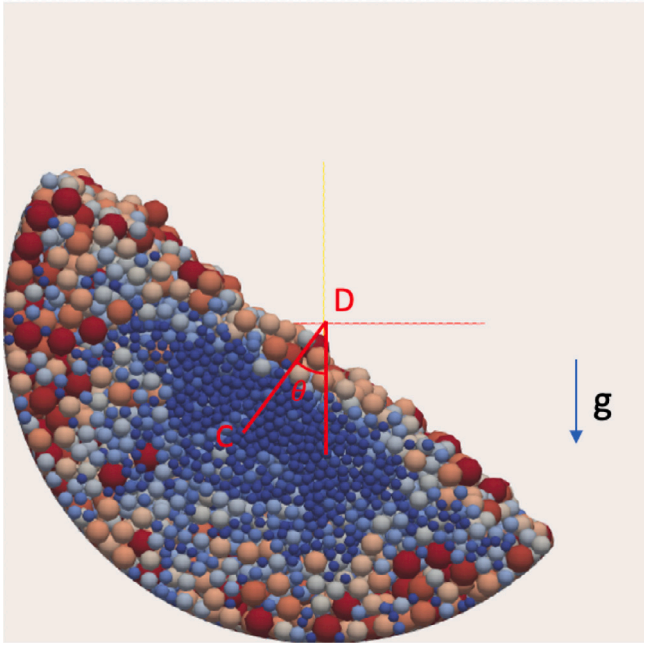

Fig. 4. Measurement of AoR of powder in the simulated rotating drum.

Measurement of the dynamic AoR. Consistently with the validating experiment, the dynamic AoR is determined by measuring the angle formed between the line connecting the drum's center C and the powder's center of mass D and the direction of gravity, see Fig. 4. In all DEM simulations, simulation time was adjusted to 30 s, and we recorded the dynamic AoR every 0.1 s.

3. Results

Data acquisition. First, we determined the period during which the dynamic AoR remained steady in the simulations. As mentioned, the time of each simulation was 30 s (2.5 - 15 full revolutions of the drum). We measured the dynamic AoR every 0.1 s for a total period of 30 s. To find the steady state of the dynamic AoR, we measured and plotted the moving standard deviation and moving mean of the dynamic AoR over time using MATLAB. The moving standard deviation represents the standard deviation computed over a specified time interval of one

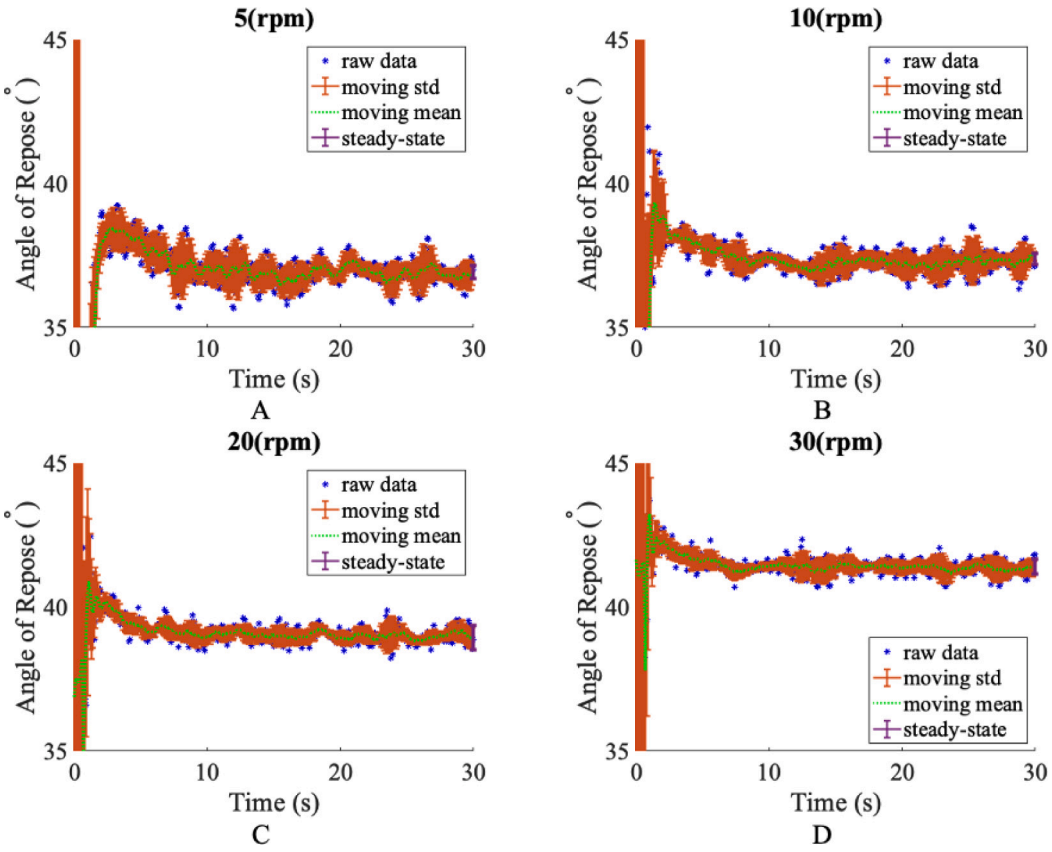

Fig. 5. AoR vs. time for different rotation speeds.

second, while the moving mean represents the average computed over the same time interval.

As shown in Fig. 5, by analyzing the plots of the moving standard deviation and moving mean, we identified a specific time interval during which the AoR appeared to exhibit a steady state. Notably, between 15 and 30 s, the moving means consistently fell within the range of the standard deviation calculated at the last second. Therefore, we confidently concluded that the AoR reached a plateau after 15 s. This observation remains valid for all the rotation speeds studied, as shown in Fig. 5 (A-D). Therefore, we performed our study utilizing the standard deviation and mean value of the dynamic AoR over the last 15 s of the simulation time.

Mathematical model. Fig. 6 gives the mean measured AoR as a function of μ_s and μ_r values for a few rotating drum speeds. It can be observed that the shape of the same-AoR level lines shown in Fig. 6 remains similar and seems to be unaffected by the flowing regime, and the Froude number. This suggests that we could find a multiplicative equation that describes the AoR in terms of particle properties, μ_s and μ_r, and rotation speed.

The following mathematical model was suggested to describe the entire array of numerical simulation results for all combinations of μ_s, μ_r, and Froude numbers:

$$AoR^{fit}(\mu_s, \mu_r, Fr) = a(1 + bFr)\left(1 + \frac{f\mu_s^2(\mu_r + c)}{(\mu_s^2 + e)(\mu_r + d)}\right) \quad (3)$$

An optimization procedure was carried out to determine the coefficients of the equation. As the objective function, the chi-square statistic [31] was used to minimize the sum of squared differences between the simulation AoR values and the corresponding values predicted by the model, normalized by the corresponding errors.

Based on this optimization procedure, the coefficients for the model equation are determined to be $a = 19.07°$, $b = 0.82$, $c = 0.11$, $d = 0.35$, $e = 0.02$, and $f = 1.37$.

Table 4
AoR at $\mu_s = 0.8$ and $\mu_r = 0.35$ and different rotation speeds.

Rotation speed (rpm)	Experiment AoR (°)	Simulation AoR (°)	Fit model AoR (°)
5	37.25 ± 0.33	36.95±0.60	36.86
10	37.94 ± 1.4	37.33±0.29	37.84
20	40.28 ± 0.67	39.12±0.22	39.79
30	42.71 ± 0.91	41.43±0.25	41.75

Fig. 7 visually demonstrates the accuracy of the model. It shows a cross-section of the fitting curve obtained from the equation for the drum rotation speed of 20 rpm (Froude number of 0.1769). One can observe a good agreement between the equation and the simulated results.

Validation. Using a rotating drum at four different rotation speeds, experimental measurements were conducted to validate the fitting equation derived from the simulation data. Table 4 illustrates the AoR of polypropylene powder for various rotation speeds we measured using image processing, as discussed earlier. A comparison was made between the experimental and model-predicted AoR values.

First, we found the μ_s and μ_r, at which the simulated AoR matches the experimental AoR. The results showed that a range of DEM parameters matches the experimental results. Therefore, we selected the physical value of $\mu_s = 0.8$ and the corresponding value of $\mu_r = 0.35$ for our validation process.

To evaluate the agreement between the fitting equation and the experimental results, we compared experimental AoR and the predicted AoR from the fitting equation at $\mu_s = 0.8$ and $\mu_r = 0.35$ for each of the four different Froude numbers in Fig. 8. A good agreement was observed between the two, demonstrating that our simulation-informed mathematical model accurately describes the system's behavior for this particular granular material.

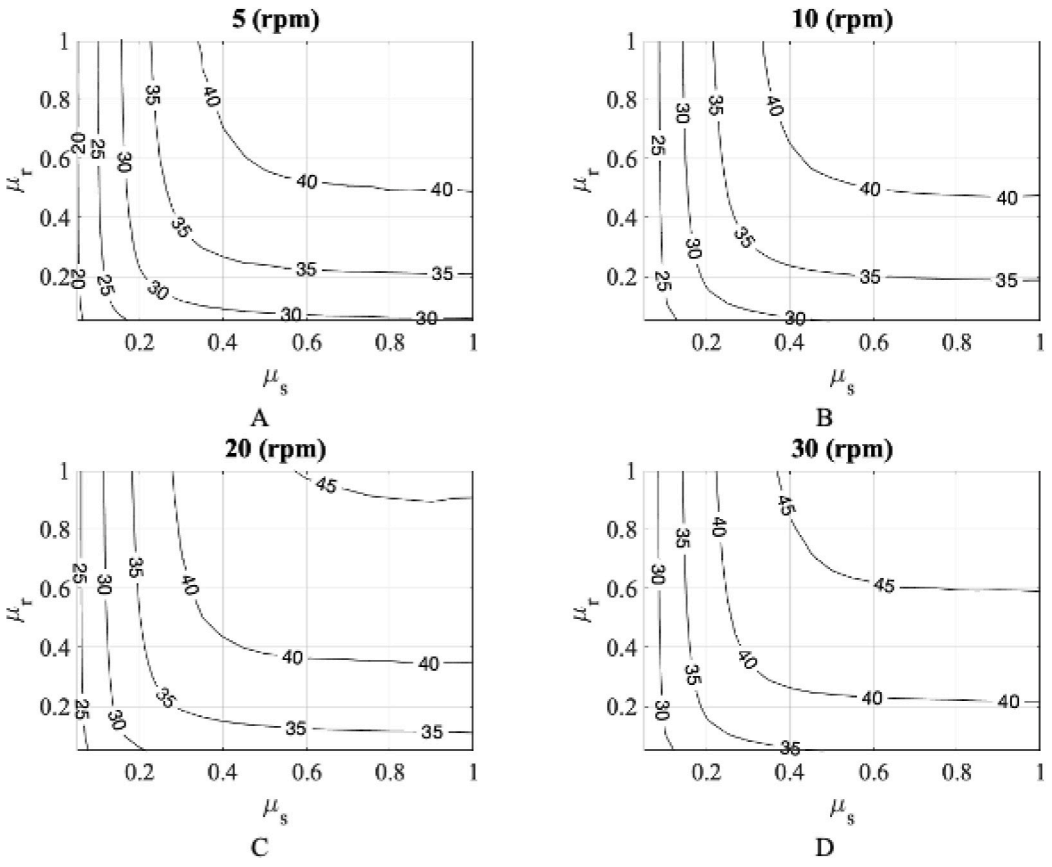

Fig. 6. Mean measured AoR as a function of material properties (μ_s and μ_r) for different rotation speeds.

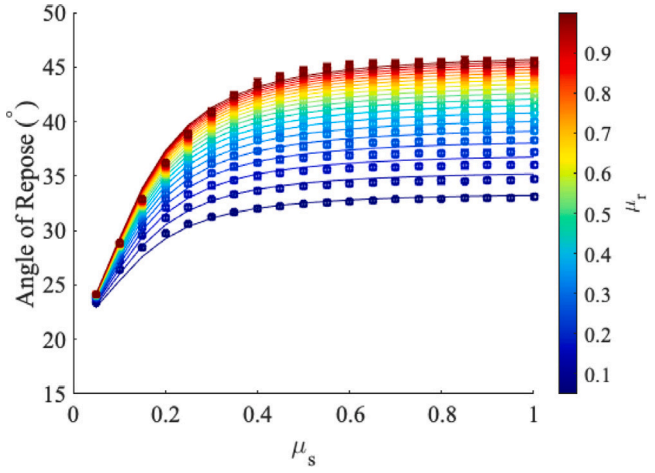

Fig. 7. Fitting curve of the derived equation (lines) and simulated AoR (markers) for Froude number of 0.1769.

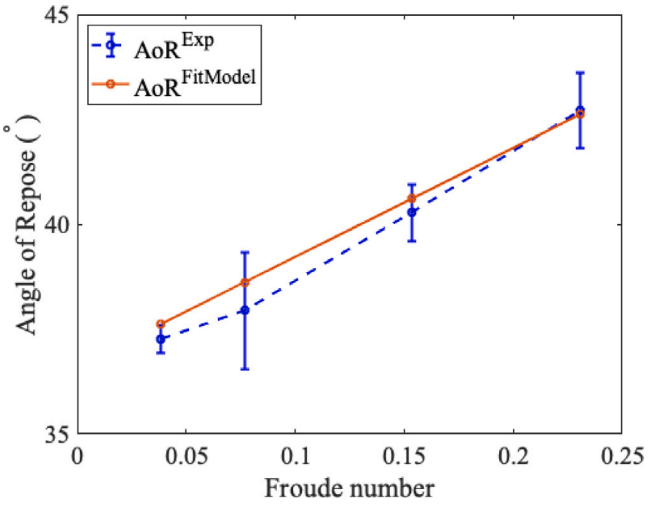

Fig. 8. Comparing experimental AoR and predicted AoR from the fitting equation.

4. Conclusions

This study aimed to examine the relationship between the measured bulk response of granular material in terms of particle properties and process conditions. In particular, we looked at the relationship between the AoR, the particle's sliding and rolling friction, and the rotating drum speed (or Froude number). Through simulations, we have derived a mathematical model that accurately describes how these parameters influence the AoR. The derived multiplicative equation implies that we can describe the effect of particle properties independently of the process parameters.

We validated the fitting model by comparing the predicted AoR and experimental measurements of the AoR in a rotating drum at various rotation speeds (or Froude numbers). A good agreement between the predicted and measured AoR was observed, confirming that our model captures the effect of operating conditions and material properties on the AoR.

The results of our study are useful for a number of industrial applications that involve processing particulates. The model can be further refined, and its applicability to specific granular processes can

be explored in future research. By improving our knowledge of granular dynamics, developing more efficient and sustainable engineering solutions in this field will be possible. However, our model is limited in applicability. This study is validated for 1 mm-sized particles. The applicability of this concept to particles outside this size range, especially 1 μm-sized particles, needs additional study. μm-sized particles may have van der Waals forces and cohesive effects that the current model does not account for. Therefore, future research should examine the model's validity across a wider range of particle sizes and include additional factors such as particle shape, particle size distribution and environmental conditions.

CRediT authorship contribution statement

Sahar Pourandi: Writing – original draft, Visualization, Validation, Methodology, Investigation, Formal analysis, Data curation, Conceptualization. **P. Christian van der Sande:** Writing – original draft, Validation, Methodology. **Thomas Weinhart:** Writing – review & editing, Writing – original draft, Supervision. **Igor Ostanin:** Writing – review & editing, Writing – original draft, Supervision.

Declaration of competing interest

The authors declare that they have no known competing financial interests or personal relationships that could have appeared to influence the work reported in this paper.

Data availability

Data will be made available on request.

Acknowledgments

This research is part of the Industrial Dense Granular Flows project that received funding from the Dutch Research Council (NWO), Netherlands in the framework of the ENW PPP Fund for the top sectors and from the Ministry of Economic Affairs in the framework of the "PPS-Toeslagregeling".

Authors sincerely thank Professor Stefan Luding and Professor Anthony Thornton for valuable discussions on the topic.

References

[1] J. Miura, K. Maeda, S. Toki, Method of measurement for the angle of repose of sands, Soils Found. 37 (2) (1997) 89–96, http://dx.doi.org/10.3208/sandf.37.2_89.

[2] H.M.B. Al-Hashemi, O.S.B. Al-Amoudi, A review on the angle of repose of granular materials, Powder Technol. 330 (2018) 397–417, http://dx.doi.org/10.1016/j.powtec.2018.02.003.

[3] F. Elekes, E.J. Parteli, An expression for the angle of repose of dry cohesive granular materials on earth and in planetary environments, Proc. Natl. Acad. Sci. 118 (38) (2021) e2107965118, http://dx.doi.org/10.1073/pnas.2107965118.

[4] GDR MiDi gdrmidi@ polytech. univ-mrs. fr http://www.lmgc. univ-montp2. fr/MIDI/, On dense granular flows, Eur. Phys. J. E 14 (2004) 341–365, http://dx.doi.org/10.1140/epje/i2003-10153-0.

[5] S.J. Linz, P. Hänggi, Effect of vertical vibrations on avalanches in granular systems, Phys. Rev. E 50 (5) (1994) 3464, http://dx.doi.org/10.1103/PhysRevE.50.3464.

[6] M.G. Kleinhans, H. Markies, S.J. de Vet, A.C. in 't Veld, F.N. Postema, Static and dynamic angles of repose in loose granular materials under reduced gravity, J. Geophys. Res. Planets 116 (E11) (2011) http://dx.doi.org/10.1029/2011JE003865.

[7] Y.C. Zhou, B.H. Xu, A.B. Yu, P. Zulli, An experimental and numerical study of the angle of repose of coarse spheres, Powder Technol. 125 (1) (2002) 45–54, http://dx.doi.org/10.1016/S0032-5910(01)00520-4.

[8] D.A. Santos, M.A. Barrozo, C.R. Duarte, F. Weigler, J. Mellmann, Investigation of particle dynamics in a rotary drum by means of experiments and numerical simulations using DEM, Adv. Powder Technol. 27 (2) (2016) 692–703, http://dx.doi.org/10.1016/j.apt.2016.02.027.

[9] R. Briend, P. Radziszewski, D. Pasini, Virtual soil calibration for wheel-soil interaction simulations using the discrete-element method, Can. Aeronaut. Space J. 57 (2011) 59–64, http://dx.doi.org/10.5589/q11-009.

[10] S.M. Derakhshani, D.L. Schott, G. Lodewijks, Micro–macro properties of quartz sand: experimental investigation and DEM simulation, Powder Technol. 269 (2015) 127–138, http://dx.doi.org/10.1016/j.powtec.2014.08.072.

[11] S. Just, G. Toschkoff, A. Funke, D. Djuric, G. Scharrer, J. Khinast, K. Knop, P. Kleinebudde, Experimental analysis of tablet properties for discrete element modeling of an active coating process, AAPS PharmSciTech 14 (2013) 402–411, http://dx.doi.org/10.1208/s12249-013-9925-5.

[12] D. Markauskas, R. Kačianauskas, Investigation of rice grain flow by multi-sphere particle model with rolling resistance, Granul. Matter 13 (2011) 143–148, http://dx.doi.org/10.1007/s10035-010-0196-5.

[13] X.Y. Liu, E. Specht, J. Mellmann, Experimental study of the lower and upper angles of repose of granular materials in rotating drums, Powder Technol. 154 (2005) 125–131, http://dx.doi.org/10.1016/j.powtec.2005.04.040.

[14] R.Y. Yang, R.P. Zou, A.B. Yu, Microdynamic analysis of particle flow in a horizontal rotating drum, Powder Technol. 130 (2003) 138–146, http://dx.doi.org/10.1016/S0032-5910(02)00257-7.

[15] R.L. Carr, Evaluating flow properties of solids, Chem. Eng. 72 (1965) 163–168.

[16] DesignerData, Polypropylene, 2024, https://designerdata.nl/materials/plastics/thermo-plastics/polypropylene-(cop.). (Accessed 19 February 2024).

[17] P.A. Cundall, O.D.L. Strack, A discrete numerical model for granular assemblies, Géotechnique 29 (1) (1979) 47–65, http://dx.doi.org/10.1680/geot.1979.29.1.47, http://www.icevirtuallibrary.com/doi/10.1680/geot.1979.29.1.47, arXiv:arXiv:1011.1669v3.

[18] T. Weinhart, L. Orefice, M. Post, M.P. van Schrojenstein Lantman, I.F. Denissen, D.R. Tunuguntla, J. Tsang, H. Cheng, M.Y. Shaheen, H. Shi, P. Rapino, E. Grannonio, N. Losacco, J. Barbosa, L. Jing, J.E.A. Naranjo, S. Roy, W.K. den Otter, A.R. Thornton, Fast, flexible particle simulations — An introduction to MercuryDPM, Comput. Phys. Comm. 249 (2020) 107129, http://dx.doi.org/10.1016/j.cpc.2019.107129.

[19] A. Di Renzo, F.P. Di Maio, Comparison of contact-force models for the simulation of collisions in DEM-based granular flow codes, Chem. Eng. Sci. 59 (3) (2004) 525–541, http://dx.doi.org/10.1016/j.ces.2003.09.037.

[20] S. Luding, Cohesive, frictional powders: contact models for tension, Granul. Matter 10 (4) (2008) 235–246, http://dx.doi.org/10.1007/s10035-008-0099-x.

[21] T. Roessler, A. Katterfeld, Scaling of the angle of repose test and its influence on the calibration of DEM parameters using upscaled particles, Powder Technol. 330 (2018) 58–66, http://dx.doi.org/10.1016/j.powtec.2018.01.044.

[22] C.M. Wensrich, A. Katterfeld, Rolling friction as a technique for modelling particle shape in DEM, Powder Technol. 217 (2012) 409–417, http://dx.doi.org/10.1016/j.powtec.2011.10.057.

[23] C++ documentation for INFINITY, C++ reference, 2024, https://en.cppreference.com/w/cpp/types/numeric_limits/infinity.

[24] G. Juarez, P. Chen, R.M. Lueptow, Transition to centrifuging granular flow in rotating tumblers: a modified froude number, New J. Phys. 13 (2011) 053055, http://dx.doi.org/10.1088/1367-2630/13/5/053055.

[25] A. Jarray, V. Magnanimo, S. Luding, Wet granular flow control through liquid induced cohesion, Powder Technol. 341 (2019) 126–139, http://dx.doi.org/10.1016/j.powtec.2018.02.045.

[26] C.J. Coetzee, Particle upscaling: Calibration and validation of the discrete element method, Powder Technol. 344 (2019) 487–503, http://dx.doi.org/10.1016/j.powtec.2018.12.022.

[27] S.C. Thakur, J.P. Morrissey, J. Sun, J.F. Chen, J.Y. Ooi, Micromechanical analysis of cohesive granular materials using the discrete element method with an adhesive elasto-plastic contact model, Granul. Matter 16 (2014) 383–400, http://dx.doi.org/10.1007/s10035-014-0506-4.

[28] Y.J. Huang, O.J. Nydal, B. Yao, Time step criterions for nonlinear dense packed granular materials in time-driven method simulations, Powder Technol. 253 (2014) 80–88, http://dx.doi.org/10.1016/j.powtec.2013.10.010.

[29] Z. Yan, S.K. Wilkinson, E.H. Stitt, M. Marigo, Discrete element modelling (DEM) input parameters: understanding their impact on model predictions using statistical analysis, Comput. Particle Mech. 2 16 (2015) 283–299, http://dx.doi.org/10.1007/s40571-015-0056-5.

[30] S. Lommen, D. Schott, G. Lodewijks, DEM speedup: stiffness effects on behaviour of bulk material, Particuology 12 (2014) 107–112, http://dx.doi.org/10.1016/j.partic.2013.03.006.

[31] F. James, Statistical methods in experimental physics, second ed., World Scientific Publishing Company, 2006, http://dx.doi.org/10.1142/6096, arXiv:https://www.worldscientific.com/doi/pdf/10.1142/6096, URL https://www.worldscientific.com/doi/abs/10.1142/6096.